Iranian Polymer Journal
18 (12), 2009, 937-946

Available online at: http://journal.ippi.ac.ir

Development of Tramadol Microparticles by Non-solvent Addition Method and their In Vitro Characterization

Muhammad Naeem Aamir* and Mahmood Ahmad

Faculty of Pharmacy and Alternative Medicine, The Islamia University of Bahawalpur, Bahawalpur-63100, Pakistan

Received 31 March 2009; accepted 18 November 2009

A B S T R A C T

New formulations of microparticles for Tramadol HCl (TmH) controlled-release were developed and evaluated. These microparticles with controlled-release characteristics were prepared by non-solvent addition technique. Ethyl cellulose (EC) a hydrophobic polymer was employed to control and extend the drug release process. Dichloromethane (DCM) was employed as solvent for polymer and paraffin oil as non-solvent which induced phase separation. Microparticles of different polymer concentrations M_1 (1:1), M_2 (1:2) and M_3 (1:3) were prepared. Among all these formulations, M_3 presented superior and desirable characteristics, i.e., 79% entrapment efficiency, good micromeritic properties, smooth morphology, and more sustained effect on cumulative release. Zero order, first order, Higuchi, Hixson-Crowell, and Korsmeyer-Peppas kinetic models were applied to assess the mechanism and pattern of drug release from microparticles. Release of TmH was best fitted to Higuchi model because it presented highest values of correlation coefficient (R^2 = 0.981) followed by zero-order kinetic model (R^2 = 0.899). FTIR, XRD, and DSC analyses ensured the chemical stability and integrity of TmH and EC in M_3 as no new bands were detected in FTIR spectra. Moreover the XRD patterns of TmH showed its reduced crystallinity and endothermic peak was observed at the glass transition temperature of EC in DSC spectra. M_3 sample was kept at 40ºC/75% RH for three months and its stability was evaluated by determining sample's in vitro release profile and drug assay. The effect of accelerated environment on its stability was not significant.

Key Words:

Tramadol;
ethyl cellulose;
stability studies;
in vitro evaluation;
kinetic models.

(*) To whom correspondence to be addressed.
E-mail: mna19bwp@yahoo.com

INTRODUCTION

Tramadol HCl (TmH) as shown in Figure 1a is a synthetic, centrally acting analgesic having bitter taste which is currently approved for use in many countries. It acts as opiate agonists, through selective binding to the μ-opioid receptor, and weak inhibition of norepinephrine and serotonin uptake [1,2]. Tramadol was treated with a sulphonic acid cation-exchange by Zhang using spray-drying method [3]. Matrix sustained release tablets of TmH were developed using xanthan and guar gum [4]. Therefore, new formulations of microencapsules of TmH using non-solvent addition techique were devolped and subjected to in vitro evaluation.

Sustained drug delivery is the most striking and challenging area in medical sciences, chemistry, materials science, pharmaceutics, and other biological sciences. Its

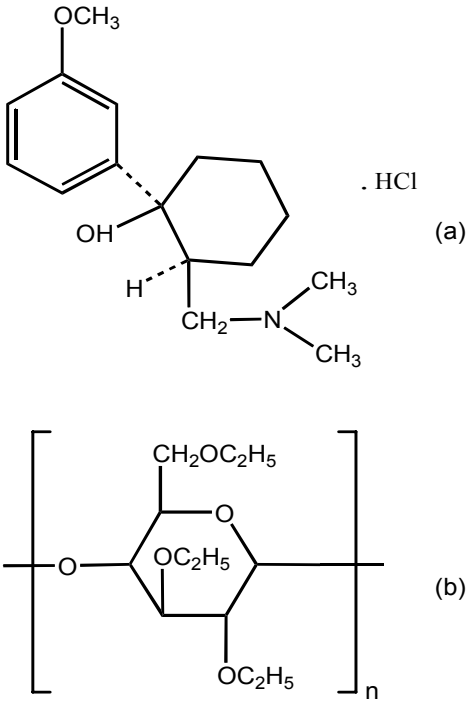

Figure 1. Structural formula of: (a) tramadol HCl and (b) ethyl cellulose.

application has resulted in the attainment of an improved quality of life and health care for human beings [5]. A large number of polymers are used to achieve oral sustained drug delivery systems. These polymers according to their origin range from simple natural polymers to semi-synthetic and synthetic polymers. According to their nature, polymers are divided into hydrophilic and hydrophobic polymers. Hydrophilic polymers include hydroxypropylmethyl cellulose (HPMC), methylcellulose (MC), and hydroxypropylcellulose (HPC). Polylactide-*co*-glycolide (PLGA) and ethylcellulose (EC) are common examples of hydrophobic polymers. EC, an ethyl ether of cellulose is a long chain polymer of β-glucose units joined together by acetal linkages (Figure 1b). Its chemical formula is $C_{12}H_{23}O_6(C_{12}H_{22}O_5)_nC_{12}H_{23}O_6$ where "n" can vary to provide a wide variety of molecular weights. It is obtained as a white granular solid by ethyl chloride treatment of soaked wood pulp in sodium hydroxide. It is an inert hydrophobic polymer and is essentially tasteless, odorless, colourless, insoluble in water, but soluble in a wide range of organic solvents [6]. It is used as a non-swellable, insoluble component in matrix or coating systems. Because of its better properties, EC was employed in this study [7].

The goal of current study was to develop a new sustained-release formulation of TmH. Plasma half-life of TmH is short and its doses are administered 3-4 times daily. Therefore, sustained-release formulation increases patient's compliance by reducing its frequent intakes. For the development of sustained-release microparticles, a unique but simple method based on non-solvent addition was developed. This method has not been reported in literature previously. First, EC was dissolved in DCM and TmH was dispersed in polymer solution. Then paraffin oil was added to induce phase separation that resulted in microparticles generations. The microparticles were then evaluated for drug release kinetics, drug-polymer interaction, and stability.

EXPERIMENTAL

Materials

Tramadol HCl (TmH) was gifted by AGP, Pakistan. Ethyl cellulose 22 cp and DCM were purchased from BDH Chemicals Limited, Poole, UK. Methanol and n-hexane were supplied by Merck, Germany. Mineral oil was purchased from Acros Organics, USA. All materials used were of analytical grade.

Preparation of Microparticles

Microencapsulation based on non-solvent addition method was employed to formulate the microparticles of TmH. One gram EC was dissolved in 10 mL of DCM. Then, 1 g of TmH was dispersed in the polymer solution. Paraffin oil was taken in burette and added to drug-polymer dispersion solution drop by drop with continuous stirring at 700 rpm till milky coloration appeared. The supernatant was decanted and n-hexane was added to wash paraffin oil. The microparticles were filtered and again washed with n-hexane and distilled water to remove paraffin oil and free drug particles from the surface of microparticles. Finally the microparticles were dried at 40ºC in an oven and stored in an air-tight glass container at room temperature for the characterization step.

Characterization of Microparticles

Size and Morphology of Microparticles

Microparticles of different formulations were observed under optical microscope (Nikon, Japan). Morphology of microparticles was studied using scanning electron microscope (Hitachi, S 3000H, Japan). Microparticles were spotted on a double-sided adhesive tape attached to an aluminium stub. Excess microparticles were removed and the stub sputter was coated with gold using a vacuum evaporator to render them electrically conductive. The coated microparticles were viewed under a scanning electron microscope at 25 kV to disclose the surface quality [8].

Product Yield

Product yield (Table 1) of the microparticles was calculated by the following equation to determine the efficiency of the process [9]:

$$Mass\ loss\ (\%) = \frac{M_0 - M_1}{M_0} \times 100$$

where,

M_0 = Initial weight of drug and polymer

M_1 = Weight of microparticles

Entrapment Efficiency

The drug content of microparticles was determined by dissolving a known weight of microparticles (M_1, M_2, and M_3) in small volume of methanol to dissolve the EC layer over the drug. To this solution, 15 mL of distilled water was added and the solution was heated to evaporate the methanol. The final volume was made to 25 mL with distilled water, filtered to remove insoluble EC, and diluted to make volume up to 100 mL with distilled water. One millilitre portion of this solution was taken and diluted to make a volume of 100 mL and analyzed by a UV-spectrophotometer at 270 nm. The absorbance of pure drug (100 mg) was also determined using the following equation. Entrapment efficiency was increased as the concentration of EC was increased (Table 1).

Entrapment efficiency = (absorbance of microparticles containing 100 mg Tramadol HCl) / (absorbance of 100 mg Tramadol HCl) × 100

In Vitro Drug Release of Microparticles

In vitro drug release of various microparticles [10] was determined using USP apparatus II. Five millimeter samples were collected at following time intervals: 0, 15, 30, 45, 60, 90, 120, 180, 240, 300, and 360 min with an automated collector after filtering through 10 μm sinter filters. All samples were diluted up to 25 mL and analyzed at 270 nm using a UV-spectrophotometer. The in vitro cumulative drug release study was conducted in triplicate.

Flow Properties of Microparticles

Tapped Density

The tap density (Table 2) of a material is basically used to investigate the packing properties of the microparticles but may also affect a number of pharmaceutical processes like flow, mixing, and tableting. The tapped density was measured by employing the conventional tapping method using 10 mL measuring cylinder and the number of tappings was fixed to 100 tappings as it was sufficient to bring about a plateau condition with microparticles. The tapped densities were calculated using the following equation [11].

Table 1. Effect of polymer concentration on the properties of microparticles.

Microparticles	Size* (μm)	Shape	Entrapment efficiency* (%)	Product yield (%)
M_1	181 ± 10.13	Spherical	63 ± 1.32	90 ± 2.23
M_2	192 ± 12.36	Spherical	71 ± 2.54	92 ± 2.56
M_3	210 ± 10.37	Spherical	79 ± 1.83	88 ± 3.18

(*) All mean values are obtained by 3 readings ± SD

Table 2. Flow properties of microparticles.

Sample	Angle of repose (degree)	Hausner's ratio*	Compressibility index* (%)	Tapped bulk density* (g/mL)	Loss bulk density* (g/mL)
M_1	28.27 ± 1.33	1.15 ± 0.01	7 ± 1.42	0.42 ± 0.01	0.26 ± 0.02
M_2	25.87 ± 2.14	1.11 ± 0.02	10 ± 2.01	0.41 ± 0.01	0.29 ± 0.02
M_3	22.48 ± 1.26	1.11 ± 0.01	9 ± 1.53	0.45 ± 0.02	0.32 ± 0.01
TmH	-	1.44 ± 0.03	29 ± 1.42	0.53 ± 0.01	0.25 ± 0.01

(*) All mean values are obtained by 3 readings ± SD

Tapped density = mass of microparticles/volume of microparticles after 100 tappings

Compressibility Index (Carr's Index)

It is an indirect measure of bulk density, size and shape, surface area, moisture content, and cohesiveness of microparticles. It is also called as Carr's index. Compressibility index (Table 2) was calculated using the following equation:

Ci = (initial volume – final volume)/(initial volume) × 100

Hausner's Ratio

The Hausner's ratio (Table 2) is another index of the flowability of the microparticles. It was calculated by the following equation:

Hausner's Ratio = volume before tapping / volume after tapping

A value < 1.2 is preferable for a free flow. However, a Hausner's ratio closer to 1 indicates good flow properties.

Angle of Repose

Angle of repose (Table 2) was measured by passing microparticles through a funnel on the horizontal surface. The height (h) of the heap formed was measured and the radius r of the cone base was also determined. The angle of repose (θ) was calculated as follows:

$$Tan\ \theta = h / r$$

Among all three formulations M_3 presented better entrapment efficiency, morphology, and flow properties. Moreover, sustained effect of M_3 was prolonged because of higher concentration of EC. Therefore, M_3 was selected for further in vitro evaluation.

Batch Reproducibility and Stability Studies

Stability studies were performed according to ICH and WHO guidelines. M_3 samples were packed in an airtight amber glass bottles. The bottles were kept at 40ºC/75% RH [12]. The samples of M_3 were withdrawn after 1, 2, and 3 months and evaluated for stability by determining in vitro release profile and drug assay [13].

Application of Kinetic Models

The dissolution data of M_3 was fitted to commonly used models, i.e., zero order, first order, Higuchi [14], Hixson-Crowell [15] and Korsmeyer-Peppas [16,17] to determine the pattern and mechanism of drug release.

Fourier Transform Infrared Spectroscopy

Drug-polymer interactions were studied by FTIR spectroscopy. The spectra were recorded for pure drug and drug-loaded microparticles using FTIR Midac 2000, USA. The samples were prepared as KBr discs. The scanning range was 500-4000 cm^{-1} and the resolution was 2 cm^{-1} [18].

X-ray Powder Diffractometry

Crystallinity of TmH, before and after encapsulation was evaluated by X-ray diffractometer (Bruker D8 Discover, Germany) using Ni-filtered CuK_α radiation source. The instrument was set up with the tube voltage of 35 kV, current of 35 mA and scanning rate of 5°/min, over a range of 8º-60° diffraction angle (2θ) range [19].

Thermal Analysis

The concurrent DSC and TGA analyses of pure drug and drug-loaded microparticles were carried out using a SDT Q600, USA. Samples (4-5 mg) were placed in aluminium pans and the lids were crimped. The analysis was performed from 25°C to 200°C temperature range, at a rate 20°C/min under nitrogen flow of 25 $mL.min^{-1}$. The instrument was calibrated with an indium standard [20-22].

RESULTS AND DISCUSSION

Size and Morphology of Microparticles

Microparticles were spherical in shape with smooth surface (Figure 2). The smooth and even surface was because of highly plasticizing nature of EC. The mean particle sizes for different formulations of microparticles are given in Table 1. An increase in microparticles size was observed parallel to the increase of the amount of EC. When the amount of EC increased the coating layer around the TmH particles became constantly thicker.

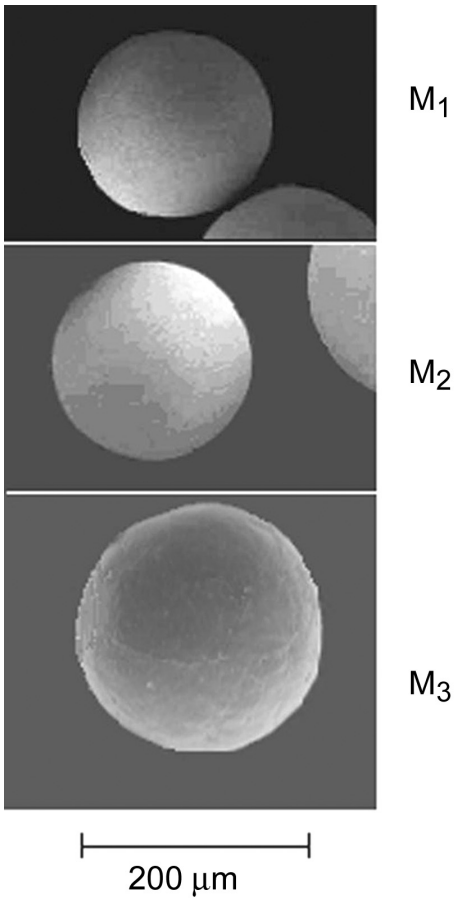

Figure 2. SEM images illustrating surface morphology of microparticles.

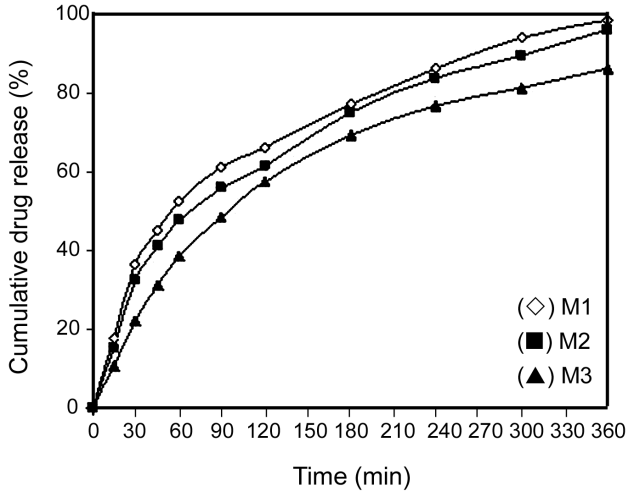

Figure 3. Release profiles from microparticles.

In Vitro Drug Release Profile of Microparticles

Increase in concentration of EC resulted in more sustained release profile. Within 2 h, approximately 66%, 61%, and 57% of drug were released from M_1, M_2 and M_3, respectively (Figure 3). Increase in the ratio of EC in the microparticles may reduce the penetration of water molecules into the polymer, thus reducing the extent of swelling of microparticles, resulting in slower release of TmH. At very high ratio of EC, the microparticles become relatively impermeable to water and give very slow release of drug, as observed in the release profile of formulation M_3.

Application of Different Kinetic Models

The drug release constant (k) and regression coefficient (R^2) were obtained for zero order, first order, Hixson-Crowell, Korsmeyer-Pappas, and Higuchi models. Drug release kinetics indicated that drug release was best explained by Higuchi's equation (Figure 4), as its plots showed the highest linearity (R^2 = 0.9813), followed by zero-order kinetic model (R^2 = 0.8999). Drug release from theophylline microparticles sustained by EC was found to follow the Higuchi model [23]. Korsmeyer's plots indicated an n value of 0.76 which was indicative of an

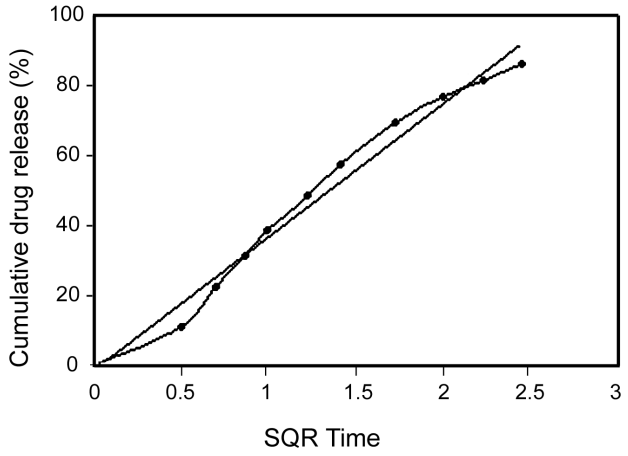

Figure 4. Higuchi kinetic model.

anomalous diffusion mechanism or diffusion coupled with erosion. Thus, the drug release was controlled by multiple mechanisms.

Anomalous release of TmH was also observed from alginate-chitosan copolymer by Acosta et al. [24]. Similar results were found with matrix tablets of nicorandil [25] and matrix tablets of theophylline [26]. Hixson-Crowell cube root law was used to plot root of drug percentage remaining in microparticles versus time. Hixson-Crowell plot indicated a change in diameter and surface area of microparticles with progress in dissolution of formulated microparticles as a function of time (Table 3).

Flow Properties of Microparticles

The loose bulk density and tapped bulk density used to assess the packability of the formulations. The pure drug was more bulky and fluffy, which was indicated by the lowest loose bulk density value. In contrast, the microparticles exhibited higher loose bulk density. The high tapped bulk density value of pure drug indicates a high inter-space between drug crystals. These results indicated good packability of the prepared spherical microparticles as compared to TmH.

The values of Carr's index, Hausner's ratio, and angle of repose were used to assess the flow and compressibility properties of the microparticles. Carr's index and Hausner's ratio of TmH have indicated extremely poor flow properties. The powder could not pass through the funnel during experiment. The poor flow of TmH could be due to its crystalline nature which posed hurdles in the uniform flow through funnel. On the other hand, all the prepared microparticles exhibited low Carr's index, indicating excellent flow properties, compressibility and angle of repose. Carr's index (compressibility index) for all the formulations indicated excellent flow, as per the scale given by Carr.

The Hausner's ratio was less than 1.25 again indicating free flow. This was further confirmed by the angle of repose values obtained for all the three formulations that were close to 30º, indicating once again the free flowing nature of the microparticles. The improved flowability and compressibility of microparticles was due to the sphericality and low size distribution. Among all the prepared formulations M_3 exhibited good micromeritic properties (Table 2).

FTIR Analysis

In the FTIR spectrum of TmH, the characteristics of aromatic CH stretching vibration about 3050 cm^{-1}, OH shoulders about 3300 cm^{-1}, aliphatic CH stretching vibration about 2900 cm^{-1}, and aromatic ring stretching vibration about 1600 cm^{-1} are observed (Figure 5 spectrum a). It is evident that only slight shift in some of the groups characteristics of drug, took place with overlapping and broadening of similar peaks (Figure 5). No new bands were detected in the spectra of microparticles, indicating no interaction between TmH and EC. Therefore, the drug

Table 3. Values of Y-equation and correlation coefficient (R^2) of M_3.

Zero order		First order		Higuchi		Hixson-Crowell		Korsmeyer-Pappas	
R^2	Y-equation	R^2	Y-equation	R^2	Y-equation	R^2	Y-equation	R^2	Y-equation
0.899	1.2601x + 3.943	0.439	0.4388x + 2.490	0.981	38.043x - 1.455	0.962	-0.3641x + 4.403	0.348	0.7658x + 3.126

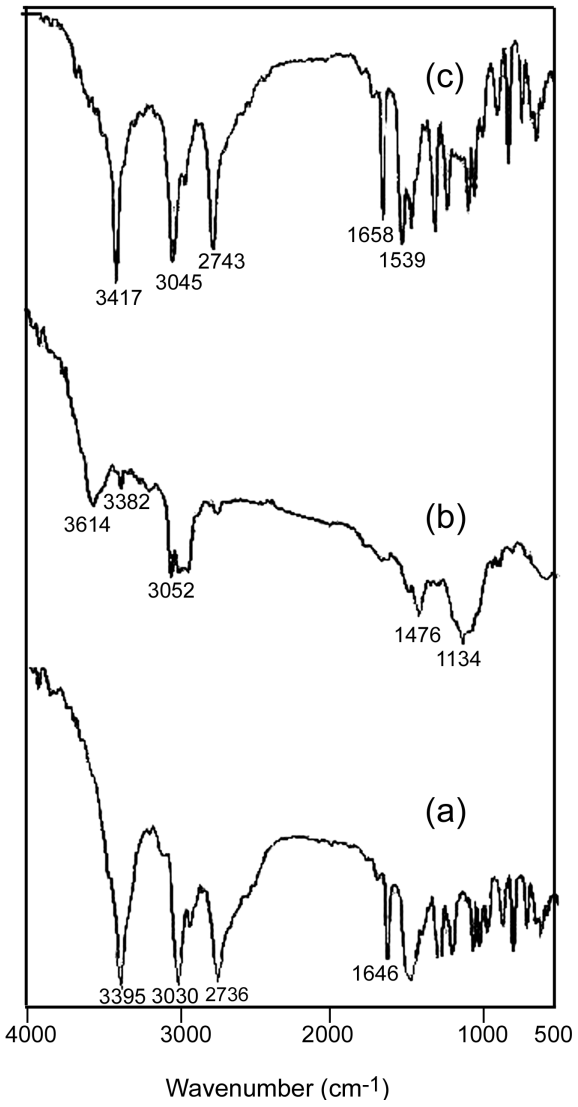

Figure 5. Fourier transform infrared spectra of: (a) tramadol HCl; (b) ethyl cellulose; (c) microparticles, M_3.

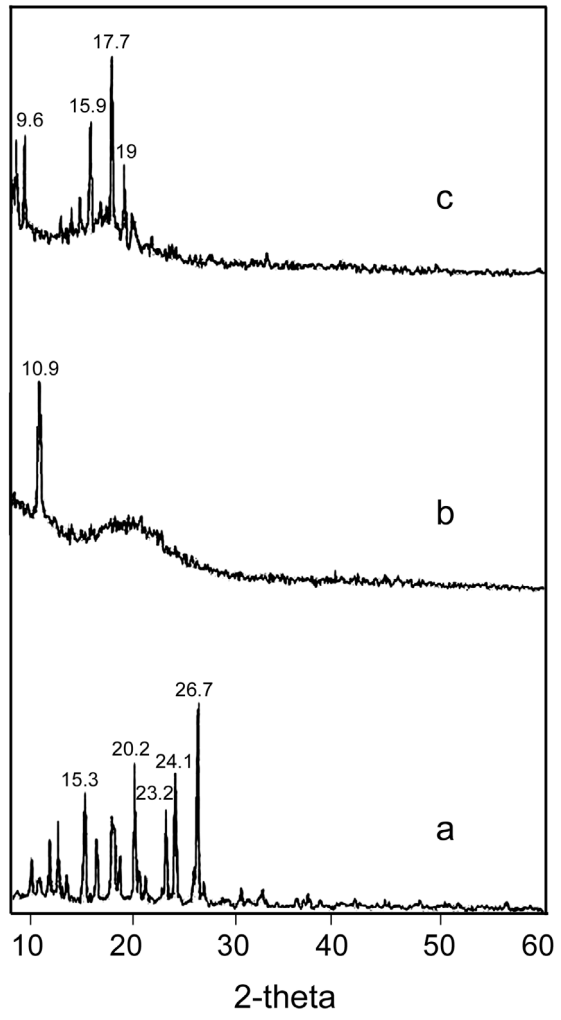

Figure 6. X-ray powder diffractometry pattern of: (a) tramadol HCl; (b) ethyl cellulose; (c) microparticles, M_3.

was chemically stable even after encapsulation. Prolongation of drug release was characterized by conjugation of EC with TmH.

XRD Determination

Every crystalline drug has a characteristic XRD pattern which can be used like fingerprint for its identification. XRD technique was employed to identify crystallographic properties of drug. TmH showed characteristic intense peaks between 2θ of 11°, 15°, 18°, 20°, 23°, 24°, and 27° due its crystalline nature. The intensity of the peaks was reduced when the drug was encapsulated in polymer which indicated the reduced crystallinity of TmH (Figure 6 pattern a). Whereas, EC presented only one shape peak at 2θ = 10.9° which indicates its amorphous regions (Figure 6 pattern b). The decrease in crystallinity also confirmed the physical stability of the drug within the polymeric microparticles [27].

Thermal Analysis

Both the melting temperature and the melting range of TmH and EC are significant. DSC analyses were conducted to explore the melting activities of drug and polymer, and therefore information about possible EC-TmH interaction was collected (Figure 7). DSC analysis showed an endothermic peak near 180°C which is an indication of melting point of

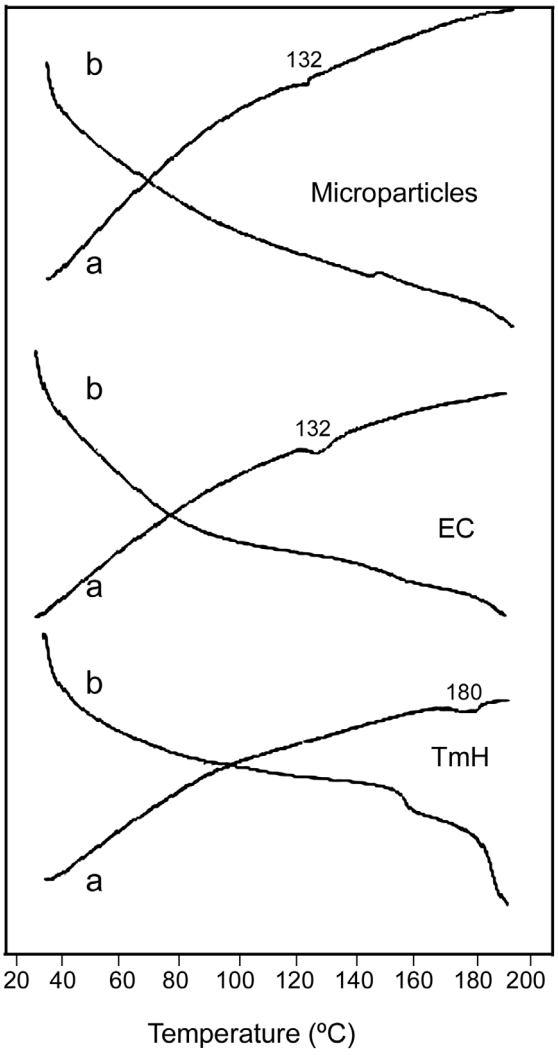

Figure 7. Thermal analysis: (a) differential scanning calorimetry; (b) thermogravimetric analysis.

TmH. Similarly, endothermic peak was observed at glass transition temperature of EC, i.e., 132°C. Decrease in ethoxy contents results in higher glass transition temperature. The glass transition temperature is dependent on ethoxy contents which were 48% in EC used in this study.

TGA analysis was conducted to supply complimentary and additional characterization information to thermal data. TGA measures the amount and rate of change in the mass of a sample as a function of temperature in a controlled atmosphere. The measurements were used to determine the thermal and/or oxidative stabilities of TmH as well as its microparticles. The quick mass loss was due to decomposition and loss of volatiles (such as moisture and/or solvent).

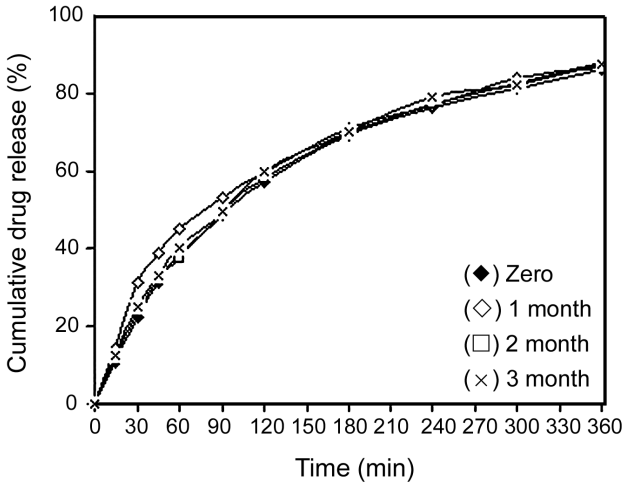

Figure 8. Release profile for three consecutive months of stability studies.

Stability Studies

EC has no aging effect while storing at accelerated storage temperatures. No significant differences in the release profiles of M_3, after storage of 1, 2, and 3 months was observed (Figure 8). Similarity factor, f_2 [28] was used to compare the difference of dissolution profile after regular interval. Values of f_2 more than 50 presented that release pattern and percentage are not significantly changed as compared to M_3, over the period of three months (Table 4). This indicates that M_3 samples are stable and can tolerate accelerated storage environment. This stability is due to coating

Table 4. Similarity factor for stability studies at accelerated conditions.

Comparison	f_2-value		
	After one month	After two months	After three months
Zero time vs. 40ºC+75% RH	66.56	67.04	66.94

of the polymer which remains stable against light, heat, oxygen, and wetness. Drug assay was within acceptable range. Drug assay was 100.00%, 98.99%, 98.21% and 96.57% after zero, one, two, and three months of stability studies, respectively.

CONCLUSION

Among the different formulations prepared in this study, M_3 (1:3) showed better release profile. Higuchi model was found to be the best model followed by first kinetic model. The drug release was controlled by more than one process such as swelling and erosion. There was no significant variation in drug assay and release profile of TmH, during stability studies of M_3 in accelerated conditions over the period of three months. FTIR, XRD, and thermal analysis supported and confirmed the compatibility of EC and TmH.

ACKNOWLEDGEMENTS

The authors are highly obliged by Ali Gohar Pharmaceuticals (Pvt.) Ltd. for providing raw materials for TmH. We also appreciate Higher Education Commission for supporting research projects in the field of pharmacy.

REFERENCES

1. Valle M, Garrido MJ, Pavon JM, Calvo R, Troconiz IF, Pharmacokinetic pharmacodynamic modeling of the antinociceptive effects of main active metabolites of Tramadol, (+)-O-desmethyl Tramadol and (-)-O-desmethyl Tramadol, in rats, *J Pharma Exp Ther*, **293**, 646-653, 2000.
2. Raffa RB, Friderichs E, Reimann W, Shank RP, Codd EE, Vaught JL, Opioid and nonopioid components independently contribute to the mechanism of action of Tramadol, an 'atypical' opioid analgesic, *J Pharma Exp Ther*, **260**, 275-85, 1992.
3. Zhang ZY, Ping QN, Xiao B, Microencapsulation and characterization of tramadol-resin complexes, *J Cont Rel*, **66**, 107-113, 2000.
4. Varshosaz J, Tavakoli N, Kheirolahi F, Use of hydrophilic natural gums in formulation of sustained-release matrix tablets of tramadol hydrochloride, *AAPS Pharm Sci Tech*, **7**, E168-E174, 2006. (DOI: 10.1208/pt070124)
5. Mashak A, Rahimi A, Silicone polymers in controlled drug delivery systems: a review, *Iran Polym J*, **18**, 279-295, 2009.
6. Shi P, Zuo Y, Zou Q, Shen J, Zhang L, Li Y, Morsi YS, Improved properties of incorporated chitosan .lm with ethyl cellulose microspheres for controlled release, *Inter J Pharma*, **375**, 67-74, 2009.
7. Dinarvard R, Zainali B, Atyabi F, Effect of formulation variable on nifedipine microspheres prepared by solvent evaporation technique, *Daru*, **9**, No 1 & 2, 2001.
8. Dolatabadi TF, Vasheghani Farahani E, Mirzadeh H, Swelling behaviour of alginate-*N,O*-carboxymethyl chitosan gel beads coated by chitosan, *Iran Polym J*, **15**, 405-415, 2006.
9. Graves RA, Pamujula S, Moiseyev R, Freeman T, Bostanian LA, Mandal TK, Effect of different ratios of high and low molecular weight PLGA blend on the characteristics of pentamidine microcapsules, *Int J Pharm*, **270**, 251-262, 2004.
10. Atyabi F, Vahabzadeh R, Dinarvand R, Preparation of ethylcellulose coated gelatin microspheres as a multiparticulate colonic delivery system for 5-aminosalicilic acid, *Iran J Pharm Res,* **2**, 81-86, 2004.
11. Shariff A, Manna PK, Paranjothy K, Manjula M, Entrapment of andrographolide in cross-linked alginate pellets. II: physicochemical characterization to study the pelletization of andrographolide, *Pak J Pharm Sci*, **20**, 1-9, 2007.
12. Kendall RA, Alhnan MA, Nilkumhang S, Murdan S, Basit AW, Fabrication and in vivo evaluation of highly pH-responsive acrylic microparticles for targeted gastrointestinal delivery, *Eur J Pharma Sci*, **37**, 284-290, 2009.
13. Rahman Z, Ali M, Khar R, Design and evaluation of bilayer floating tablets of captopril, *Acta Pharm*, **56**, 49-57, 2006.
14. Higuchi T, Mechanism of sustained action medication, theoretical analysis of rate of release of solid drugs dispersed in solid matrices, *J Pharm*

Sci, **52**, 1145-1149, 1963.
15. Hixson AW, Crowell JH, Dependence of reaction velocity upon surface and agitation: I-theoretical consideration, *Ind Eng Chem*, **23**, 923-931, 1931.
16. Korsmeyer RW, Gumy R, Doelker E, Buri P, Peppas NA, Mechanism of solute release from porous hydrophilic polymer, *Int J Phar*, **15**, 25-35, 1983.
17. Peppas NA, Analysis of Fickian and non-Fickian drug release from polymers, *Pharm Acta Helv*, **60**, 110-111, 1985.
18. Bhise KS, Dhumal RS, Chauhan B, Paradkar A, Kadam SS, Effect of oppositely charged polymer and dissolution medium on swelling, erosion, and drug release from chitosan matrices, *AAPS Pharm Sci Tech*, **8**, Article 44, 2007.
19. Li Z, Miao Z, Wang L, Liu J, Dai Y, Bai W, Preparation and adsorption performance of starch microspheres towards Cu^{2+}, Co^{2+}, and Ni^{2+}, *Iran Polym J*, **17**, 735-744, 2008.
20. Wang Z, Hou X, Mao Z, Ye R, Mo Y, Finlow DE, Synthesis and characterization of biodegradable poly(lactic acid-*co*-glycine) via direct melt copolymerization, *Iran Polym J*, **17**, 791-798, 2008.
21. Kaya I, Koca S, Synthesis, characterization, thermal properties and conductivity of oligo-4-[(2-methoxyphenylimino)methyl]phenol, *Iran Polym J*, **18**, 25-35, 2009.
22. Nokhodchi A, Maghsoodi M, Hassanzadeh D, An improvement of physicomechanical properties of carbamazepine crystals, *Iran J Pharm Res*, **6**, 83-93, 2007.
23. Lavasanifer A, Ghalandari R, Ataei Z, Zolphaghari ME, Mortazavi SA, Microencapsulation of theophylline using ethylcellulose: in vitro drug release and kinetic modeling, *J Microencap*, **14**, 91-100, 1997.
24. Acosta N, Aranaz I, Peniche C, Heras A, Tramadol release from a delivery system based on alginate-chitosan microparticles, *Macromol Biosc*, **3**, 546-551, 2003.
25. Reddy KR, Mutalik S, Reddy S, Once-daily sustained-release matrix tablets of nicorandil: formulation and in vitro evaluation, *AAPS Pharm Sci Tech*, **4**, E61, 2003.
26. Fassihi RA, Ritschel WA, Multiple layer, direct compression controlled release system: in vitro and in vivo evaluation, *J Pharm Sci*, **82**, 750-754, 1993.
27. Li B, Wang L, Li D, Chiu YL, Zhang Z, Shi J, Chen XD, Mao Z, Physical properties and loading capacity of starch-based microparticles crosslinked with trisodium trimetaphosphate, *J Food Eng,* **92**, 255-260, 2009.
28. Moore JW, Flanner HH, Mathematical comparison of dissolution profiles, *Pharm Tech*, **20**, 64-74, 1996.